

Divergent transcriptional states and kinetics of circulating tumor-infiltrating lymphocyte repertoires with highly homologous T-cell receptor sequences in a patient during immunotherapy

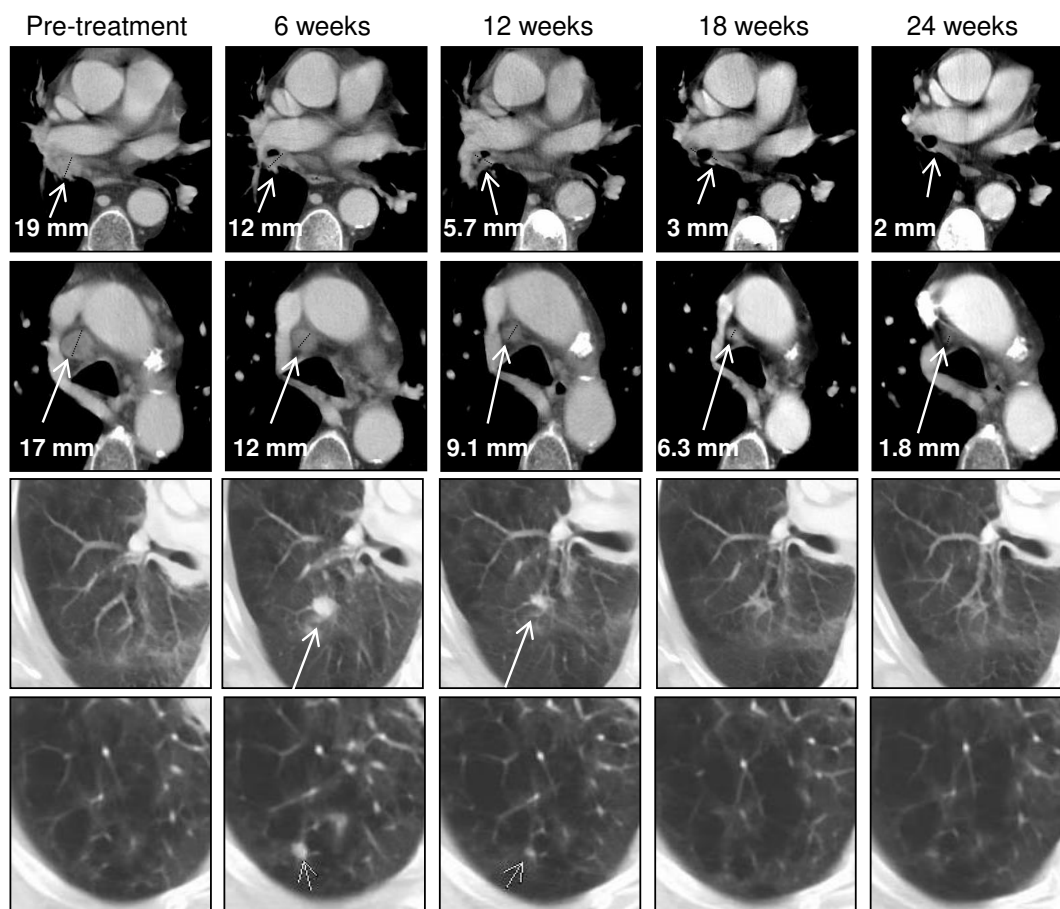
Kajihara *et al.*

Supplementary Information

Supplementary Figures 1-11

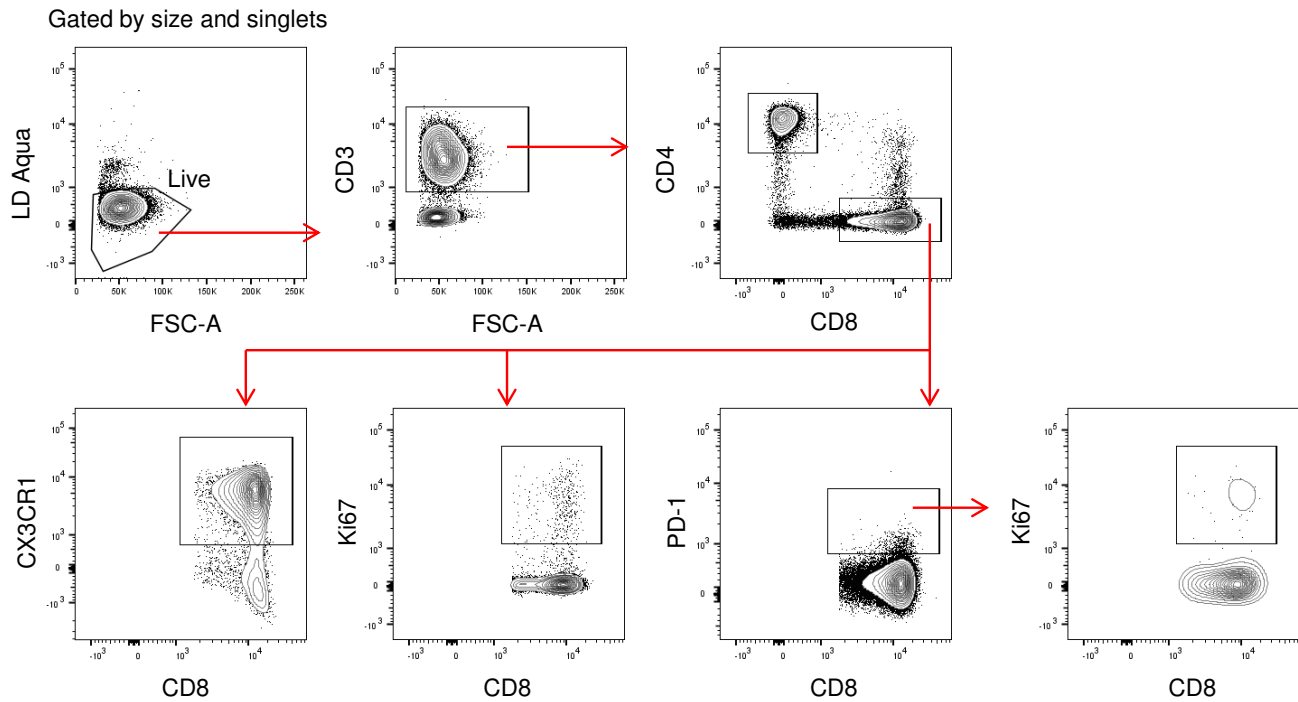
Supplementary Tables 1

Supplementary Materials and Methods



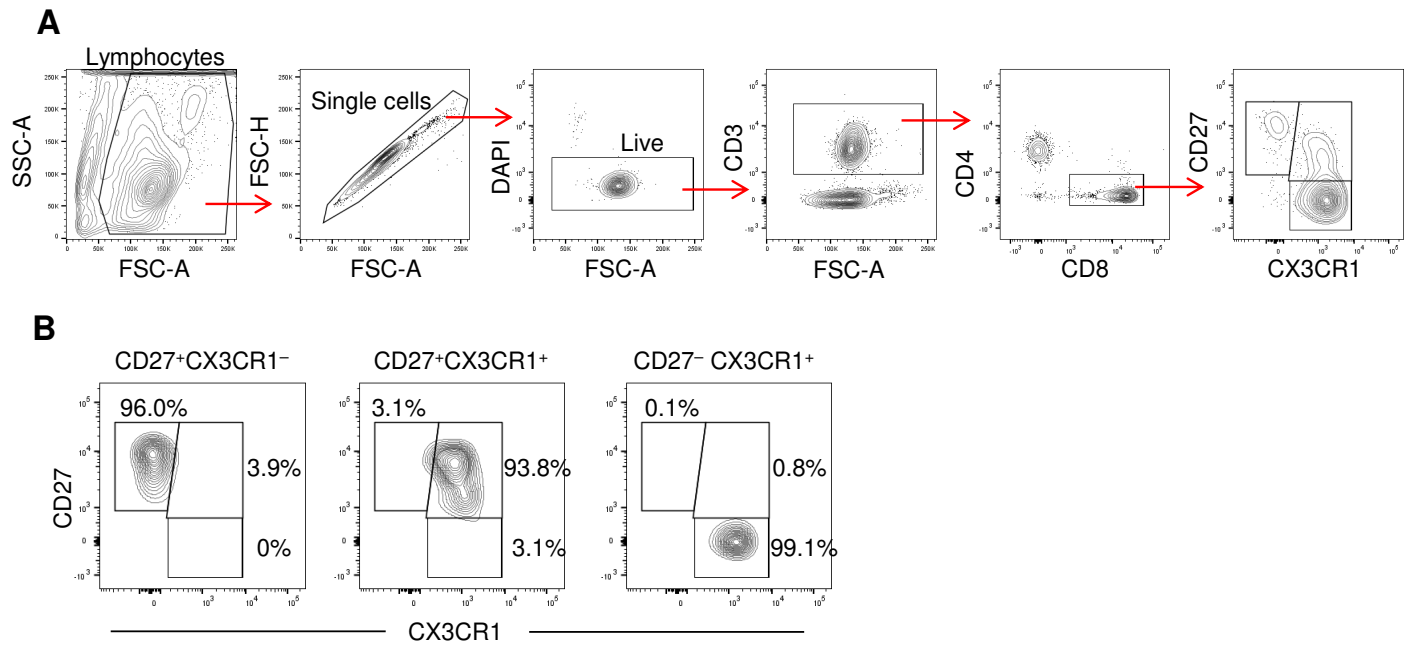
Supplementary Figure 1.

67-year-old male with Stage IIIB (T2N3M0) NSCLC (squamous cell carcinoma) was treated with anti CTLA-4/PD-1 therapy (ipilimumab and nivolumab). PD-L1 expression in the pre-treatment tumor specimen was 2%. The patient had a partial response, and was on treatment until 24 weeks after initiation of the therapy when he was found to have a progression. No immune-related adverse events were reported. Contrast-enhanced cross-sectional imaging obtained at prior to and during treatment is shown.



Supplementary Figure 2: Expression of CX3CR1 and Ki67 in a NSCLC patient treated with anti-CTLA-4/PD-1 therapy. Related to Figure 1.

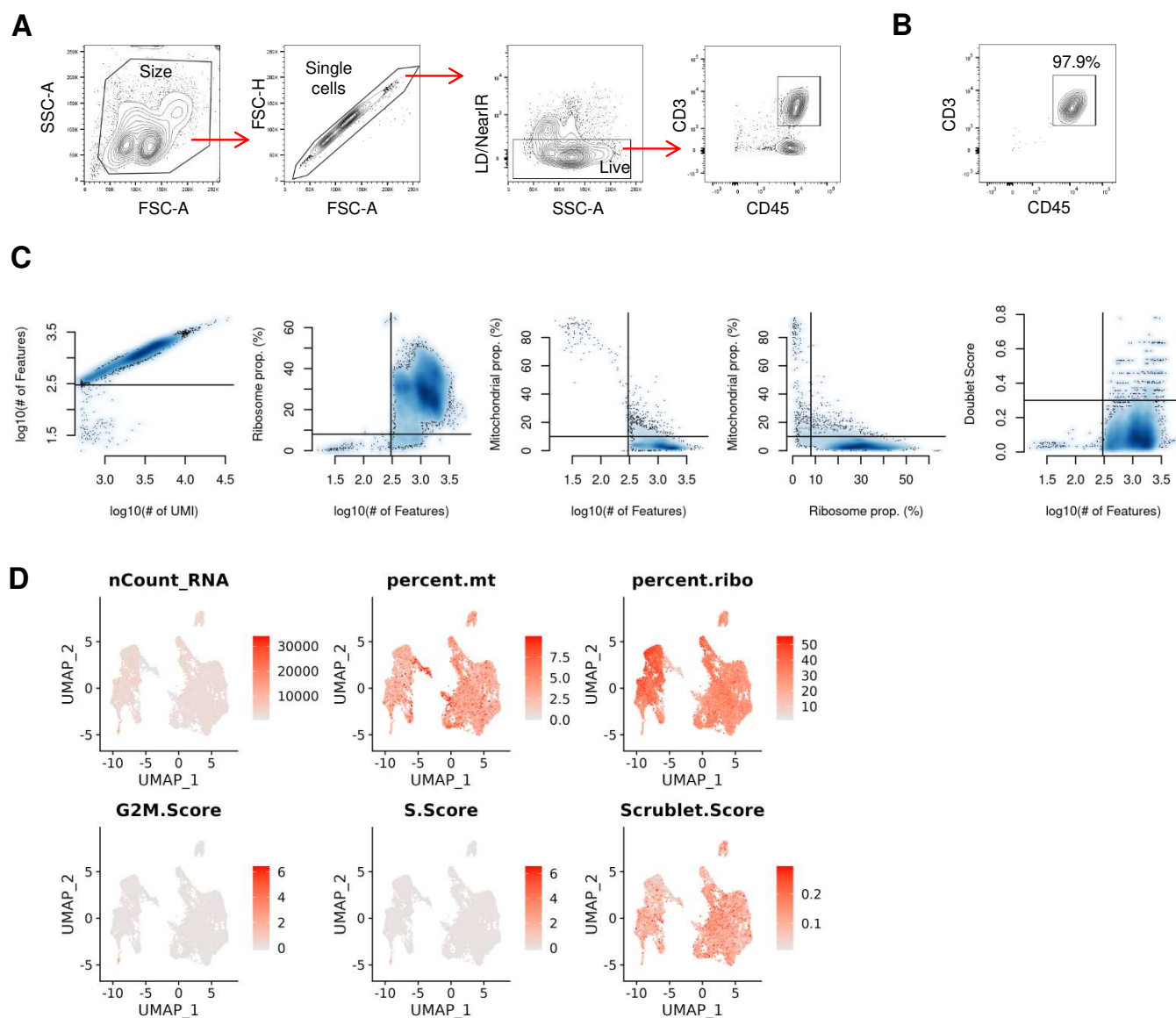
Gating strategy of identifying single live CX3CR1⁺, Ki67⁺, and Ki67⁺PD-1⁺CD8 T cells from cryopreserved peripheral mononuclear blood cells.



Supplementary Figure 3: Related to Fig. 1C

A Gating strategy of identifying single live CD27⁺CX3CR1⁻, CD27⁺CX3CR1⁺, and CD27⁻CX3CR1⁺ cells from cryopreserved peripheral mononuclear blood cells for TCR sequencing (TCR-seq).

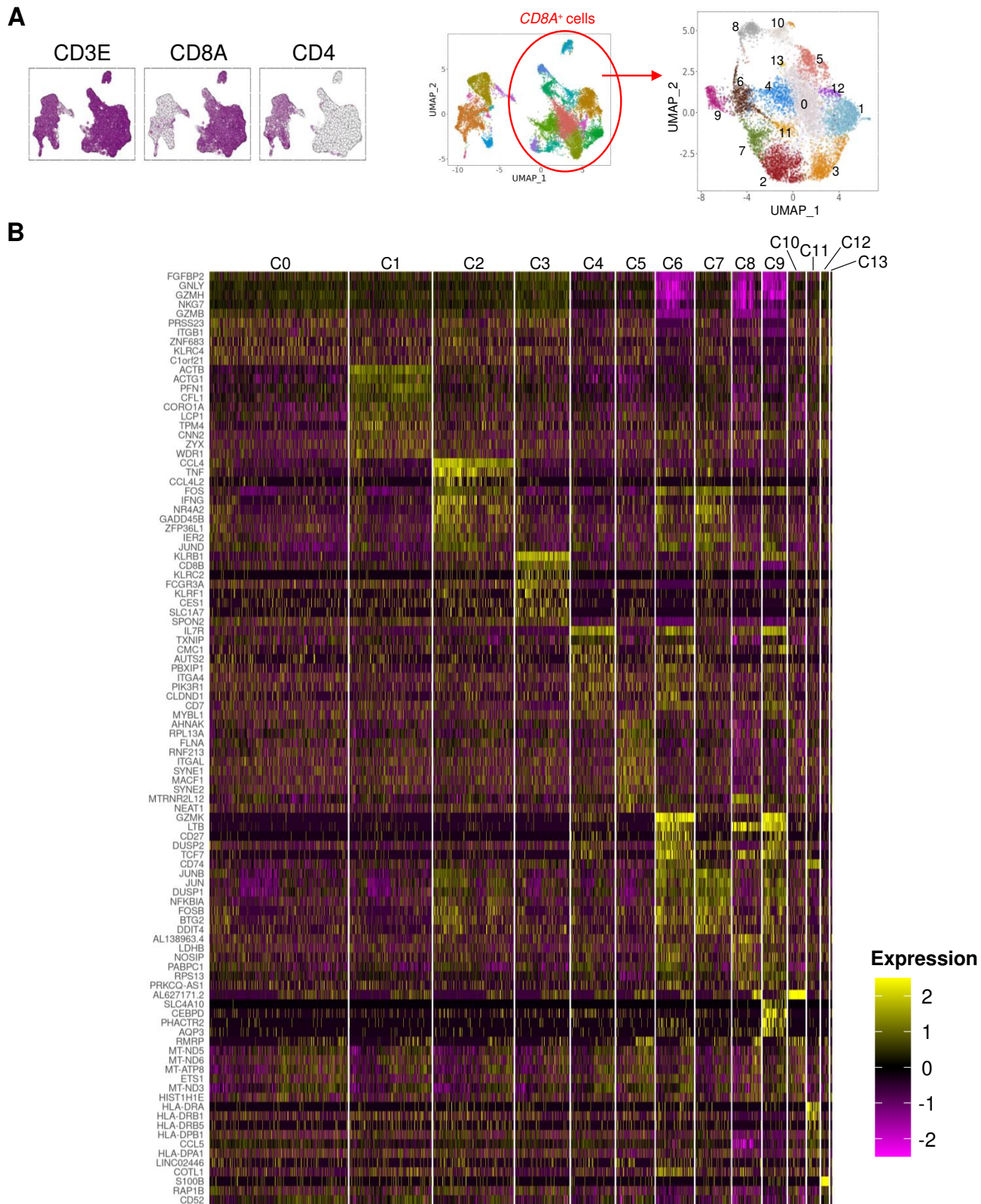
B Flow cytometric plots showing the frequency of CD27⁺CX3CR1⁻, CD27⁺CX3CR1⁺, and CD27⁻CX3CR1⁺ cells after flow-sort.

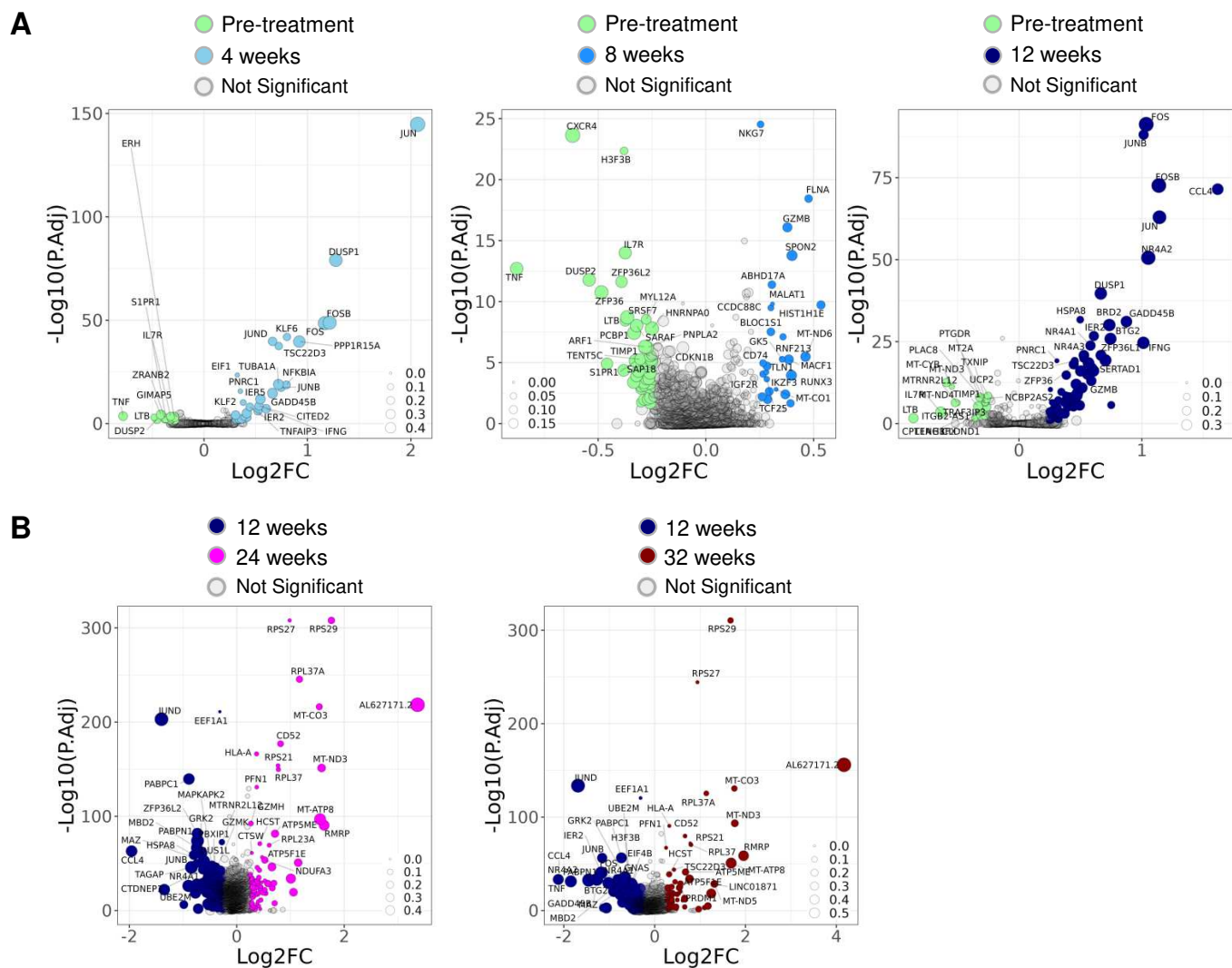


Supplementary Figure 4: Single-cell RNA/TCR sequencing (scRNA/TCR-seq) quality assessment.

Related to Fig. 2 and 3.

A Gating strategy of identifying single live CD45⁺CD3⁺ cells from cryopreserved peripheral mononuclear blood cells for scRNA/TCR-seq. **B** Representative flow cytometric plots showing the frequency of CD45⁺CD3⁺ cells after flow-sort. **C** Scatterplots depicting total features, counts, doublet scores, mitochondrial content and ribosomal content across all cells prior to filtering. Filtering thresholds applied are shown. **D** Distribution of quality control metric scores across cells.



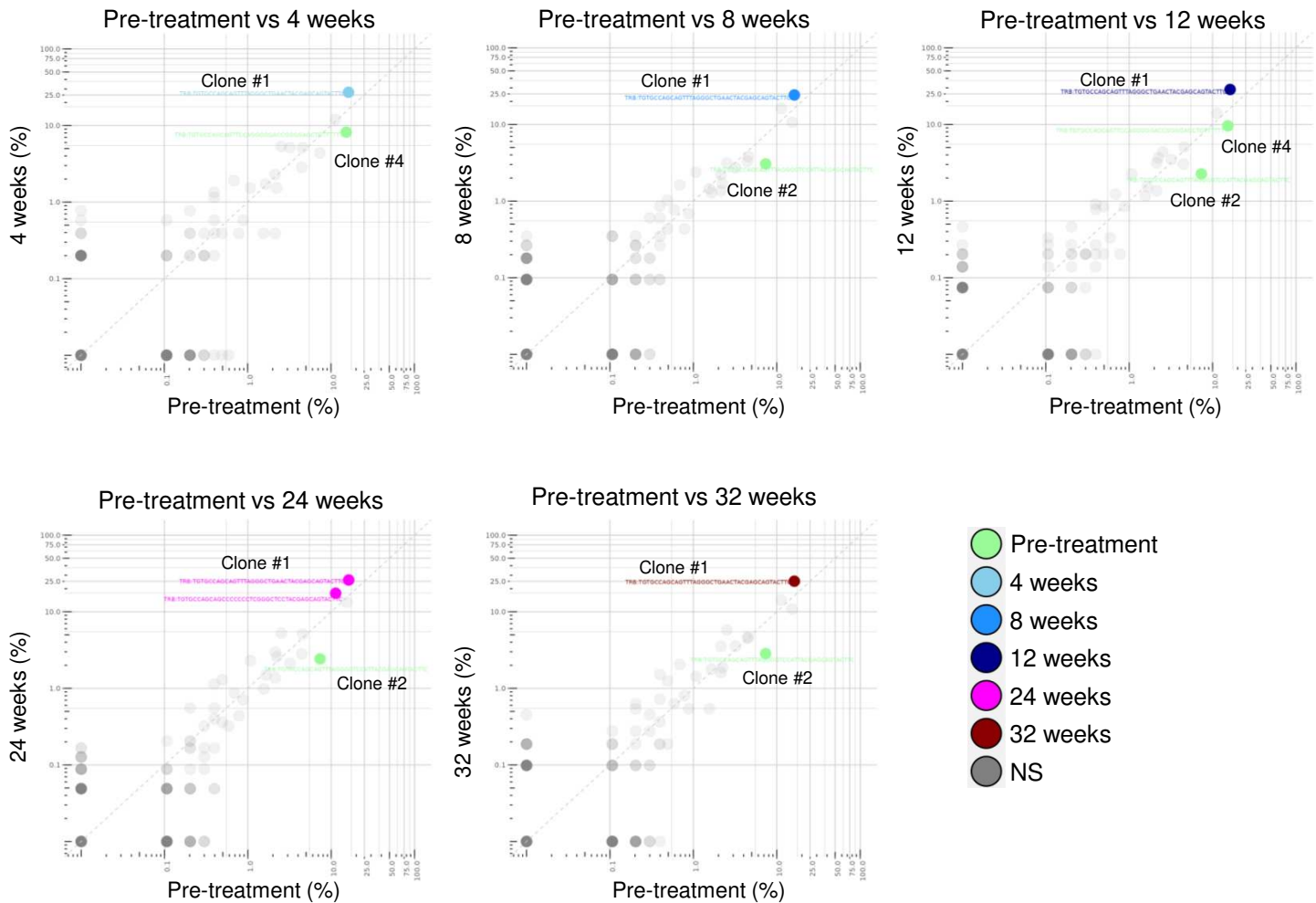


Supplementary Figure 6. Differential gene expression of circulating *CD8A+* T cells before and during ICI treatment. Related to Figure 2F and Supplementary Data 2A-E.

A Volcano plots showing enrichment differentially expressed genes in *CD8A+* T-cell subsets, pre-treatment vs. 4 weeks (left), pre-treatment vs. 8 weeks (middle) and pre-treatment vs. 12 weeks (right).

B Volcano plots showing enrichment differentially expressed genes in *CD8A+* T-cell subsets, 12 vs 24 weeks (left) and 12 vs. 32 weeks (right).

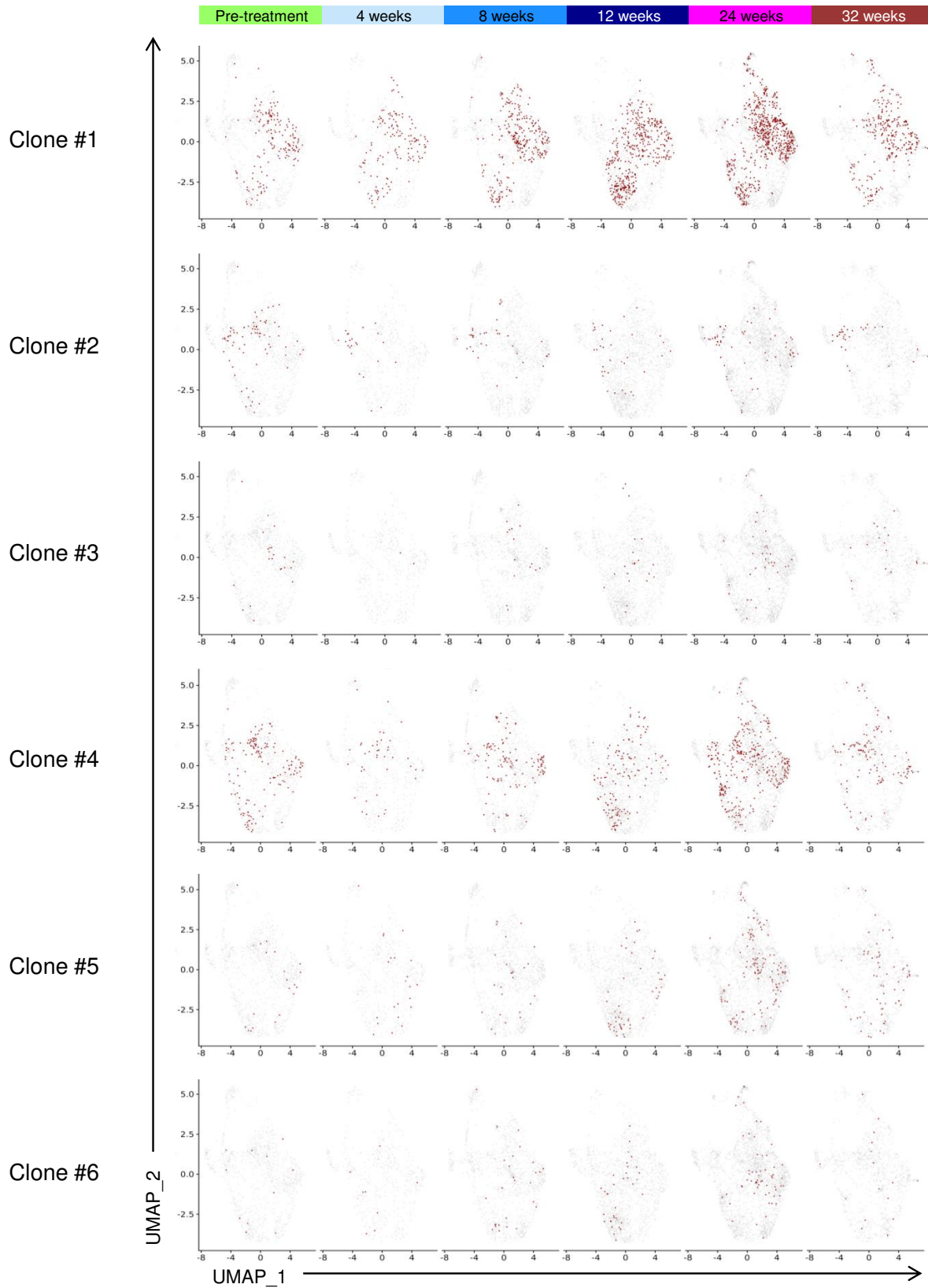
A, B The numbers in the plots indicates delta detectable fraction.



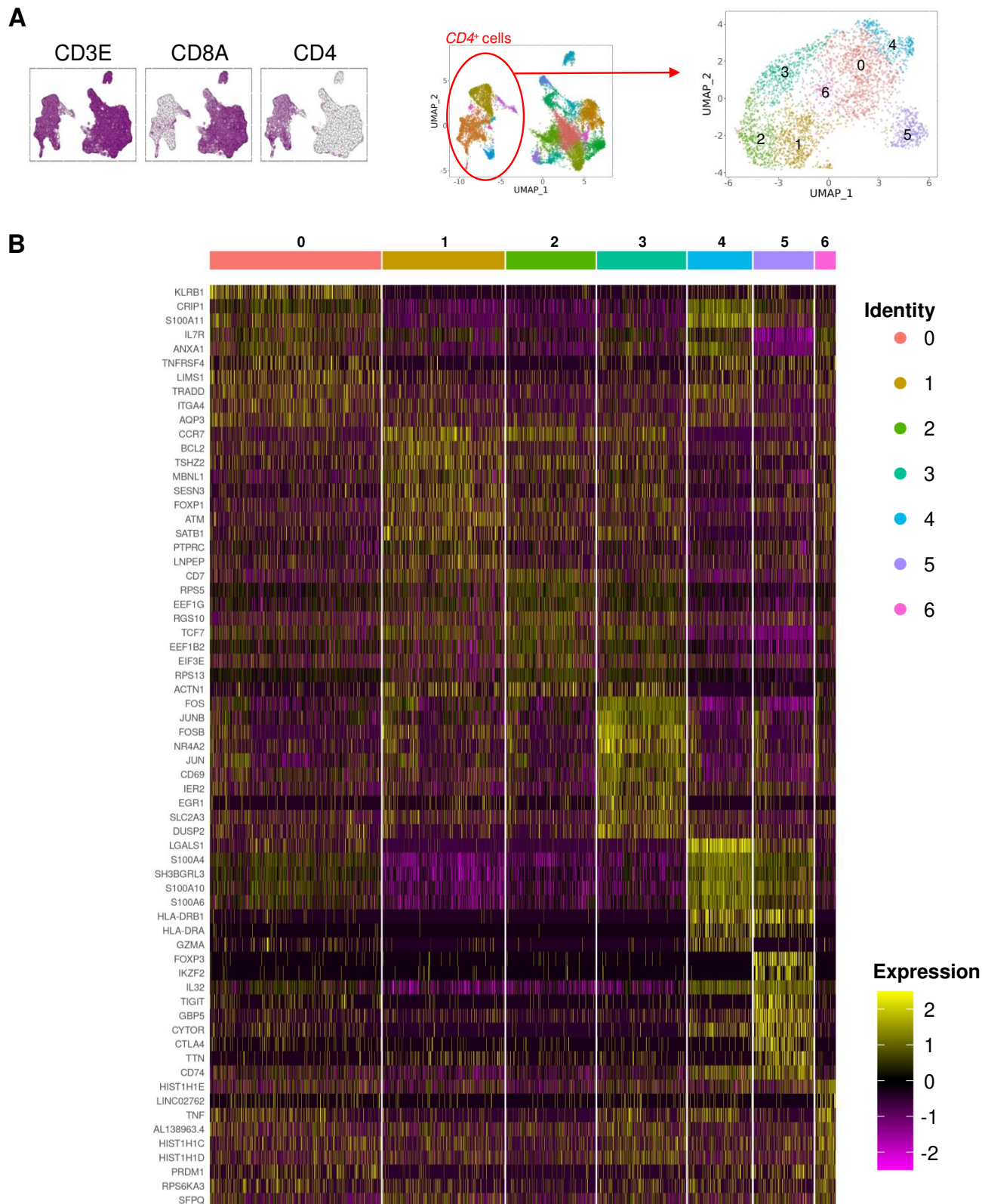
Supplementary Figure 7. Clonal expansion of circulating $CD8A^+$ TIL-TCRs during ICI treatment.

Related to Figure 3 and Supplementary Data 6A-E.

Identification of clonally expanded or contracted $CD8A^+$ T-cell repertoires (TRB) on-treatment at 4, 8, 12, 24 and 32 weeks vs. pre-treatment.



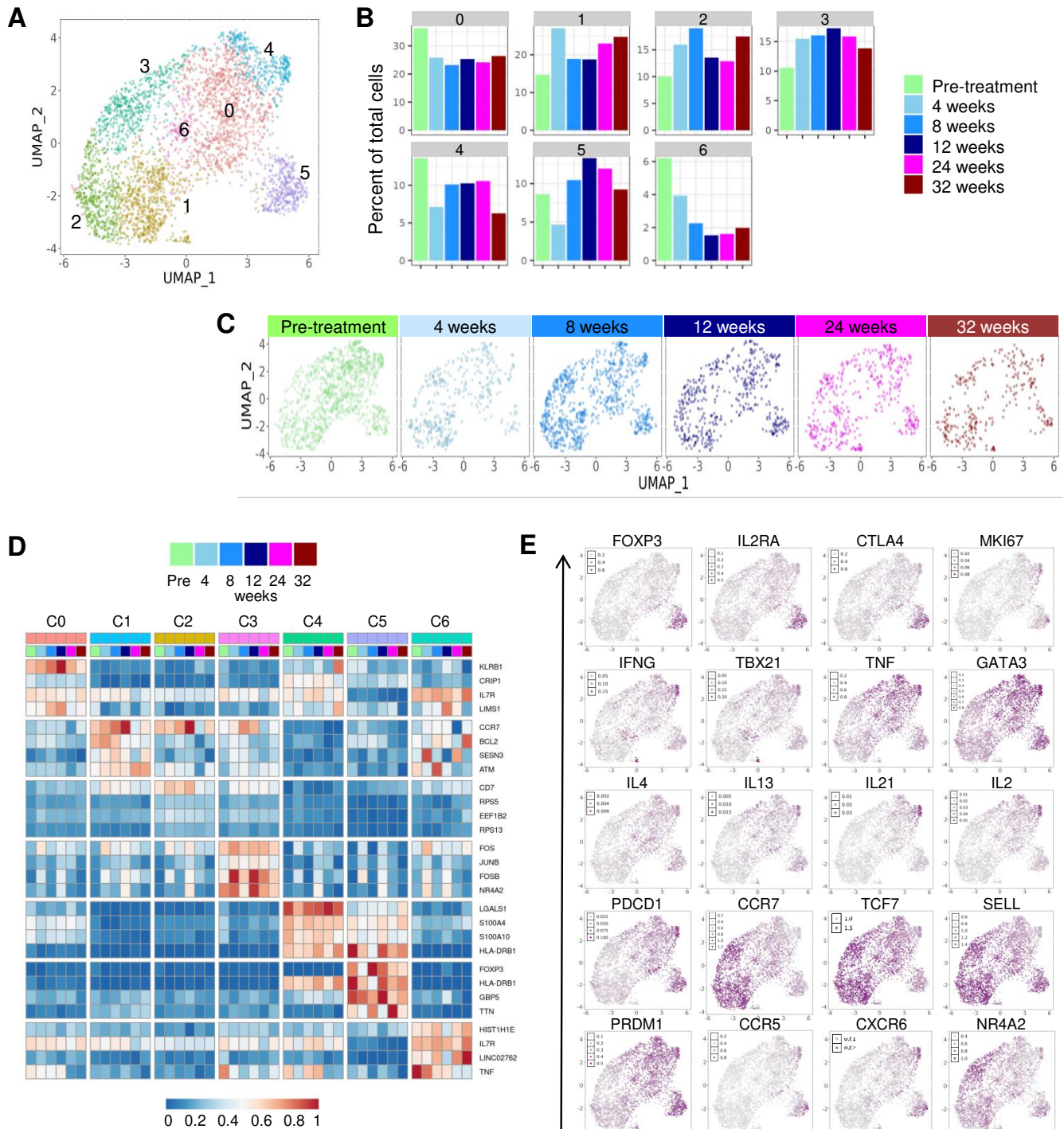
Supplementary Figure 8. Differential gene expressions of circulating $CD8A^+$ TIL-TCR clones #1-6 in Table 1 during ICI treatment. UMAP plots for each clone at different time points during immunotherapy.



Supplementary Figure 9. Analysis of peripheral blood CD45⁺CD3⁺CD4⁺ cells by scRNA/TCR-seq. Related to Supplementary Figures 9-10 and Supplementary Data 8.

A UMAP plots from merged treatment data of exclusively peripheral blood CD45⁺CD3⁺CD4⁺ cells.

B Heatmap of all cells showing the expression levels of the 14 most discriminative genes per cell type (in rows) across all the identified cell populations (in columns). Gene expression in each clusters are also listed in Supplementary Data 8. Color-code layout: scale of purple to yellow; from lowest expression to highest expression.



Supplementary Figure 10. Single-cell profiling of CD4⁺ T cells in longitudinal blood samples from an NSCLC patients treated with anti-CTLA-4/PD-1 therapy.

A UMAP plots of CD4⁺ T-cell subsets. **B** and **C** The frequency of each CD4⁺ T-cell cluster is assessed (**B**), and UMAP plots are generated (**C**) to visualize the clusters in peripheral blood at different time points as indicated.

D Heatmap displaying normalized expression of selected genes in PB CD4⁺ T-cell clusters. **E** Expression plots of indicated genes in PB CD4⁺ T-cell clusters. Expression levels are color-coded: gray, not expressed; purple, expressed.

Supplementary Table 1. Antibodies and other reagents for flow cytometric analysis.

ANTIBODY	FLUOROPHORE	CLONE	VENDER
CD3	FITC	UCHT-1	BioLegend
CD4	PE	RPA-T4	BD Biosciences
CD4	BUV395	SK3	BD Biosciences
CD8	APC-eFluor 780	RPA-T8	Thermo Fisher Scientific
CD45	V500	HI30	BD Biosciences
PD-1	PE	MIH4	BD Biosciences
CD27	PE-Cy7	O323	Thermo Fisher Scientific
CX3CR1	APC	2A9-1	BioLegend
KI-67	BV421	B56	BD Biosciences
	DAPI	N.A.	Thermo Fisher Scientific
	LIVE/DEAD™		
	Fixable Aqua Dead	N.A.	Thermo Fisher Scientific
	Cell Stain Kit		
	Near IR Viability	N.A.	Thermo Fisher Scientific
	Kit		

Supplementary Materials and Methods

Study design, patients, specimen collection and data reporting.

Written informed consent was obtained from the patient for the collection and storage of blood samples, analysis of archived tumor tissue, and review of clinical records, imaging studies, and laboratory findings. The clinical response to ipilimumab and nivolumab was assessed as the best response according to the immune-related RECIST (irRECIST)¹ within 12 weeks, as described previously.² Clinical samples were prospectively collected and selected based on their availability during the study period, 2017-2021. No statistical methods were used to determine sample size. This study was reviewed and approved by the Institutional Review Board of the Roswell Park Comprehensive Cancer Center (approval number: I 188310) in accordance with the Declaration of Helsinki.

Peripheral blood mononuclear cell (PBMC) preparation, flow cytometry and cell sorting.

Isolation and storage of PBMCs were performed as previously described.^{2,3}

Cryopreserved PBMC samples were treated with 50ul of Fc block with human IgG (12 mg/ml, Sigma) or Human TruStain FcX (BioLegend) for 15 min, followed by staining with 50 µL of FACS buffer (2% FBS in PBS) for 15 min with the antibodies described in **Supplementary Table 1**. Samples were acquired using LSRFortessa (BD Biosciences) or sorted using BD FACSAria (BD Biosciences), and data were analyzed using FlowJo software v10.1.5 (FlowJo LLC).

scRNA/TCR-seq

Sample preparation and scRNA/TCR-seq library generation.

The scRNA-seq was performed in two batches. The flow-sorted cells were stained with a unique hashtag antibody (TotalSeq-A0251 to A0254 anti-human hashtag 1 to 4 antibody, BioLegend). Sorted samples with different hashtag antibodies were mixed together in the same tube at a cell concentration of 700-1,000 cells/ μ L in 10% FBS RPMI, and scRNA/TCR-seq was performed using the standard protocol for the Chromium single-cell 5' kit v2 (10x Genomics, Inc.) as described previously.³ After sequencing libraries passed standard quality control metrics, the libraries were sequenced on Illumina NovaSeq6000 S1 100cycle v1.5 kits with the following read structure: read1:26, read2:90, index 1:10, and index 2:10. Libraries were sequenced to obtain a read depth greater than 16,000 reads/cell for the gene expression (GEX) libraries and greater than 4,000 reads/cell for the V(D)J-enriched T Cell libraries.

Raw data processing, quality control, and subsequent analyses.

Raw sequence data demultiplexing, barcode processing, alignment (GRCh38), and filtering for true cells were performed using the Cell Ranger Single-Cell Software Suite (v6.0.0), yielding 18,887 cells with a mean of 29,235 reads/cell (85.4% mapping rate), median of 1,313 genes/cell, 18,579 total unique detectable genes, and 3,148 median UMI counts/cell. Sample demultiplexing from detected hashtag antibody-associated sequences was performed by k-medoid clustering of centered log-ratio normalized counts to define a negative population distribution and using a 0.99 quantile threshold of this distribution to assign cell positivity implemented in Seurat (v4).⁴ Cells classified as positive for more than one sample were considered ambiguous and removed, leaving 14,896 cells for subsequent analyses (pretreatment,

2,437 cells; 4 weeks, 1,199 cells; 8 weeks, 2,699 cells; 12 weeks, 2,525 cells; 24 weeks, 3,945 cells; 32 weeks, 2,091 cells). Seurat was used to perform cell quality metric determination (e.g., mitochondrial and ribosomal protein gene read mapping, number of reads, and features), filtering, normalization, and downstream analyses as previously described.^{5 6} Scrublet⁷ was used to score cells for potential doublets, and cells with score > 0.3 removed. After quality control assessment, 14,044 high-quality cells (pre-treatment, 2,323 cells; 4 weeks, 1,133 cells; 8 weeks, 2,559 cells; 12 weeks, 2,422 cells; 24 weeks, 3,688 cells; 32 weeks, 1,919 cells) were included in the downstream analyses. VDJ annotations derived from Cell Ranger were analyzed using scRepertoire⁸ and custom scripts. Differential TCRB clonotype abundance was determined using Fisher's exact test.

TCR-seq

TCR β CDR3 clonotypes in DNA from formalin-fixed, paraffin-embedded (FFPE) tumor biopsy samples obtained within 30 days from the initiation of the treatment were profiled using the ImmunoSEQ immune profiling platform at the survey level (Adaptive Biotechnologies) and analyzed using the LymphoSeq package and custom scripts in the R statistical software environment to evaluate repertoire characteristics; the vegan package was used to assess the level of similarity (Morisita-Horn Index) between repertoires as previously described.^{2 3 6}

Data availability

Raw and processed scRNA/TCR-seq data supporting the findings of this study were deposited in the National Center for Biotechnology Information Gene Expression Omnibus

(NCBI GEO) under accession number GSE266035. All data generated and/or analyzed during the current study are available from the corresponding author upon reasonable request.

Statistical analysis

Statistical analysis was performed using unpaired or paired t-tests for comparisons between two groups. All tests were 2 sided and $P < 0.05$ was considered statistically significant. Data are presented as the mean \pm SEM. Statistical analysis was performed using GraphPad Prism 10.1.2 (GraphPad Software).

References

1. Seymour L, Bogaerts J, Perrone A, et al. iRECIST: guidelines for response criteria for use in trials testing immunotherapeutics. *Lancet Oncol* 2017;18(3):e143-e52. doi: 10.1016/S1470-2045(17)30074-8 [published Online First: 2017/03/02]
2. Yamauchi T, Hoki T, Oba T, et al. T-cell CX3CR1 expression as a dynamic blood-based biomarker of response to immune checkpoint inhibitors. *Nature communications* 2021;12(1):1402. doi: 10.1038/s41467-021-21619-0 [published Online First: 2021/03/05]
3. Abdelfatah E, Long MD, Kajihara R, et al. Predictive and Prognostic Implications of Circulating CX3CR1(+) CD8(+) T Cells in Non-Small Cell Lung Cancer Patients Treated with Chemo-Immunotherapy. *Cancer Res Commun* 2023;3(3):510-20. doi: 10.1158/2767-9764.Crc-22-0383 [published Online First: 20230330]
4. Butler A, Hoffman P, Smibert P, et al. Integrating single-cell transcriptomic data across different conditions, technologies, and species. *Nat Biotechnol* 2018;36(5):411-20. doi: 10.1038/nbt.4096 [published Online First: 2018/04/03]
5. Makino K, Long MD, Kajihara R, et al. Generation of cDC-like cells from human induced pluripotent stem cells via Notch signaling. *Journal for immunotherapy of cancer* 2022;10(1) doi: 10.1136/jitc-2021-003827

6. Oba T, Long MD, Keler T, et al. Overcoming primary and acquired resistance to anti-PD-L1 therapy by induction and activation of tumor-residing cDC1s. *Nature communications* 2020;11(1):5415. doi: 10.1038/s41467-020-19192-z [published Online First: 2020/10/29]
7. Wolock SL, Lopez R, Klein AM. Scrublet: Computational Identification of Cell Doublets in Single-Cell Transcriptomic Data. *Cell systems* 2019;8(4):281-91.e9. doi: 10.1016/j.cels.2018.11.005 [published Online First: 2019/04/08]
8. Borcharding N, Bormann NL, Kraus G. scRepertoire: An R-based toolkit for single-cell immune receptor analysis. *F1000Res* 2020;9:47. doi: 10.12688/f1000research.22139.2 [published Online First: 2020/12/27]